Polyhouse microclimate optimisation, fogging efficiency and plant photosynthesis measurement

1. Introduction

Sun-seed APV Private Ltd. was in searching for an organization capable of supporting meaningful, science-driven projects. The team discovered Vigyan Ashram—an NGO renowned for its, project-based approach to science education and rural development. They were inspired by blogs and reports detailing about the real-life projects and scientific data collected by student fellows at Vigyan Ashram. Recognizing that this was a place where their work could be taken seriously, Sun-seed reached out to Vigyan Ashram to initiate collaborative projects.

Project Description

1.1 Plant Photosynthesis Measurements

Plant photosynthesis measurement involves quantifying the rate at which plants convert carbon dioxide into organic compounds through photosynthesis under varying environmental conditions. Using instruments such as the Licor 6800 Portable Photosynthesis System, parameters like CO_2 assimilation, stomatal conductance, and transpiration rate are recorded. By following standardized protocols, including A–Ci curves, light-response curves, and temperature-response measurements, it is possible to derive key photosynthetic parameters such as Vcmax, Jmax, Rd25, and α. These parameters are essential for understanding the physiological performance of plants and for input into mechanistic crop growth models.

1.2 Plant Architecture Measurements

Plant architecture measurement focuses on capturing the structural and morphological traits of plants that define their form and growth pattern. Key traits include internode length, phyllochron, leaf insertion angles, leaf dimensions, curvature, and branching patterns. Measurements are taken manually at multiple stages across the plant's growth cycle to track developmental changes from germination to senescence. These data form the basis for constructing accurate plant models in simulation platforms such as Helios, enabling the study of growth dynamics, light interception, and yield potential under various environmental and management conditions.

1.3 Fogging Efficiencies and Microclimate Measurements

Different types of foggers are available in the market, each having distinct cooling efficiencies in terms of both **water consumption** and the **rate of temperature reduction** achieved during operation. However, not all the sprayed water contributes to evaporative cooling. Excess water that settles on crop leaves increases leaf wetness, which in turn promotes pest and disease incidence. The efficiency of fogging systems is also strongly influenced by the **humidity** and **temperature** conditions inside the polyhouse.

Therefore, it is necessary to establish an appropriate monitoring infrastructure capable of collecting relevant data to support the selection of suitable foggers, considering both **local climatic conditions** and the **investment capacity** of growers. To address this need, the **third objective of the proposal** was set as:

"Construction of a polyhouse facility equipped for comparative testing of different fogger types under variable climatic conditions, with respect to cooling performance and water-use efficiency."

Accordingly, a polyhouse of **35 m² floor area** and **156 m³ volume** was constructed. Three commercially available fogger systems were procured for evaluation:

- **4-way fogger**
- **Super fogger**
- **Netafim fogger**

These foggers were systematically tested under different climatic conditions to determine:

1. Cooling rate (temperature drop with time), and
2. Efficiency with respect to water consumption.

1.4 Fogger clogging Measurements

When the **aperture of foggers is reduced**, the **droplet size decreases**, which improves evaporative cooling efficiency. However, this simultaneously increases the risk of **clogging**, thereby demanding more frequent maintenance. Clogging in foggers generally arises due to:

- **Foreign particles** such as dust or organic matter carried with the water supply.
- **Salt precipitation**, particularly of calcium and magnesium salts, associated with temporary and permanent water hardness.
- **Biological growth**, such as algae, whose cells and fibrous residues obstruct fogger outlets.

To address these limitations, the **next objective of the project** was defined as:

"Generation of experimental data for designing a robust water-treatment system capable of supplying foggers with minimal maintenance requirements."

This report therefore presents the **experiments conducted**, the **data collected**, and their **interpretation**, with the aim of establishing water-treatment guidelines suitable for sustained fogger operation in polyhouse environments.

1.5 Treatment against Cooling pad clogging

In fan-pad polyhouse cooling systems, a common limitation arises due to the continuous circulation of water over the cooling pads. Prolonged wetting creates a favorable environment for algae growth, leading to the formation of a greenish layer on the pad surface. This layer gradually clogs the pad pores, obstructs airflow, and significantly reduces the overall cooling efficiency of the system.

To address this challenge, the next objective is to develop a water-treatment strategy aimed at preventing algal growth before the water reaches the cooling pads. This can be achieved by dosing the circulating water with suitable anti-algal or disinfectant chemicals in safe concentrations. Such treatment will help maintain the porosity of cooling pads, ensure efficient air–water contact, and thereby sustain the effectiveness and longevity of the cooling system.

2. Methodology, Procedure and Conclusion

2.1 Plant Photosynthesis Measurements

Plant Photosynthesis

Photosynthesis is the process by which plants convert light energy into chemical energy, forming sugars that drive growth and development. In this process, **carbon dioxide (CO_2)** from the atmosphere enters the leaf through microscopic pores known as **stomata**. Once inside, CO_2 diffuses into the mesophyll cells and reaches the chloroplasts, where it is incorporated into organic molecules via the Calvin–Benson cycle.

Stomata not only control CO_2 entry but also regulate water loss through **transpiration**. The opening and closing of stomata balance the plant's need for CO_2 uptake with the necessity to conserve water. This regulation is critical, as stomatal conductance directly affects photosynthetic efficiency.

Light provides the energy to power the **light-dependent reactions** in the chloroplast's thylakoid membranes. Photons excite electrons in chlorophyll, initiating electron transport that generates ATP and NADPH. These molecules fuel the **light-independent reactions** (Calvin–Benson cycle), where CO_2 is fixed into sugars.

To mathematically describe and quantify the biochemical limitations of photosynthesis, we use the **Farquhar–von Caemmerer–Berry (FvCB) model**, commonly referred to as the **Farquhar Model**. This mechanistic model integrates the influence of CO_2 availability, light intensity, and the biochemical capacities of the leaf to predict the rate of photosynthesis. It considers three potential limitations:

1. **Rubisco-limited photosynthesis** – limited by the maximum rate of carboxylation (**Vcmax**).
2. **Light-limited photosynthesis** – limited by the electron transport capacity (**Jmax**).
3. **Triose phosphate utilization (TPU) limitation** – limited by the capacity to use the products of photosynthesis.

In our work, we use **A–Ci curves, light-response curves, and temperature-response data** collected with the Licor 6800 to fit the Farquhar model. The fitting process, implemented through the *PhoTorch* package, provides parameters such as **Vcmax**, **Jmax**, **Rd25**, and **α**, along with temperature dependencies. These parameters serve as physiological inputs to our crop growth simulations in Helios, allowing us to link measured leaf-level photosynthetic performance to whole-plant growth predictions.

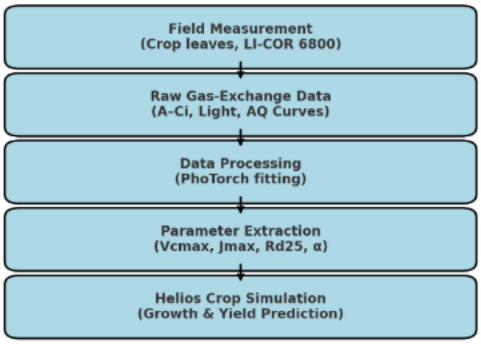

Data Collection and Processing using PhoTorch

Physiological measurements were conducted on four target crops — **Turmeric (Curcuma longa)**, **Strawberry (Fragaria × ananassa)**, **Senna alexandrina**, and **Cucumber (Cucumis sativus)** — following the standardized gas-exchange measurement protocol outlined in *PhoTorch: a robust and generalized biochemical photosynthesis model fitting package based on PyTorch*. Measurements were taken using the **LI-COR 6800 Portable Photosynthesis System**, which records parameters such as CO_2 assimilation rate, stomatal conductance, transpiration rate, and leaf temperature.

In addition to routine measurements for **A–Ci curves** (CO_2 response curves) and light-response curves, **AQ curves** were recorded multiple times throughout the day to capture the **diurnal variation in photosynthetic performance**. This approach helped determine the optimal time window for data collection, as measurements taken too late in the day showed reduced accuracy due to plants entering a physiological "rest" phase, often referred to as "falling asleep."

Protocol overview – For A–Ci measurements, leaves were clamped in the LI-COR chamber under controlled temperature, humidity, and light. CO_2 concentration was varied in a stepwise manner from low to high (and sometimes vice versa), with sufficient equilibration time at each step to stabilize gas-exchange readings. Light-response curves were obtained by adjusting light intensity in defined increments under saturating CO_2. All measurements were replicated on healthy, fully expanded leaves for each crop to ensure representativeness.

Data processing with PhoTorch – The collected gas-exchange data were processed using PhoTorch on GitHub. This Python-based package uses deep learning capabilities from PyTorch to fit the **Farquhar–von Caemmerer–Berry (FvCB) photosynthesis model** and its associated temperature-response equations. The software extracts key photosynthetic parameters including **Vcmax** (maximum carboxylation rate), **Jmax** (maximum electron transport rate), **Rd25** (day respiration at 25 °C), and **α** (quantum yield). These parameters form the physiological basis for our crop growth modeling in Helios, linking measured leaf-level photosynthetic capacity to simulated whole-plant growth and yield potential.

2.1.1 Crop 1 – Turmeric

Gas-exchange measurements for Turmeric were carried out to generate both **A–Ci curves** (CO_2 response curves) and **AQ curves** (light response curves) under controlled conditions. These datasets allow us to quantify the photosynthetic capacity of the crop and evaluate how it responds to varying environmental conditions.

A–Ci Curves – The figure below shows the variation in net photosynthetic rate (A) with intercellular CO_2 concentration (Ci) for leaves measured at **three different temperatures** while keeping all other chamber parameters constant. These curves are essential for estimating biochemical parameters such as **Vcmax** and **Jmax** using the Farquhar model, enabling us to

assess how temperature influences the carboxylation and electron transport capacities of Turmeric leaves.

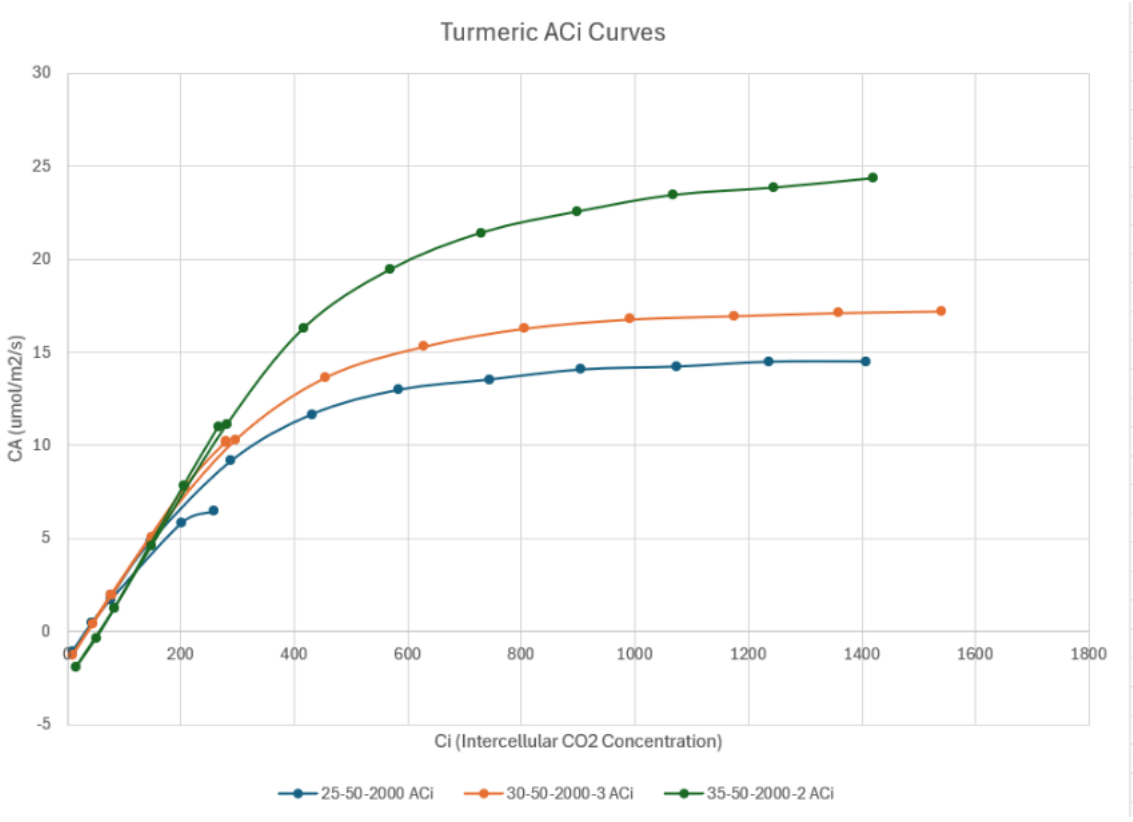

Fig.1

Aci Curves Turmeric

AQ Curves – The light response curves (AQ curves) represent the variation in photosynthetic rate with incident photosynthetically active radiation (PAR). The figure below presents three AQ curves obtained at different temperatures under saturating CO_2, allowing us to evaluate how light use efficiency and maximum photosynthetic rates change with leaf temperature. This information also informs the optimal light and temperature combinations for maximizing Turmeric productivity.

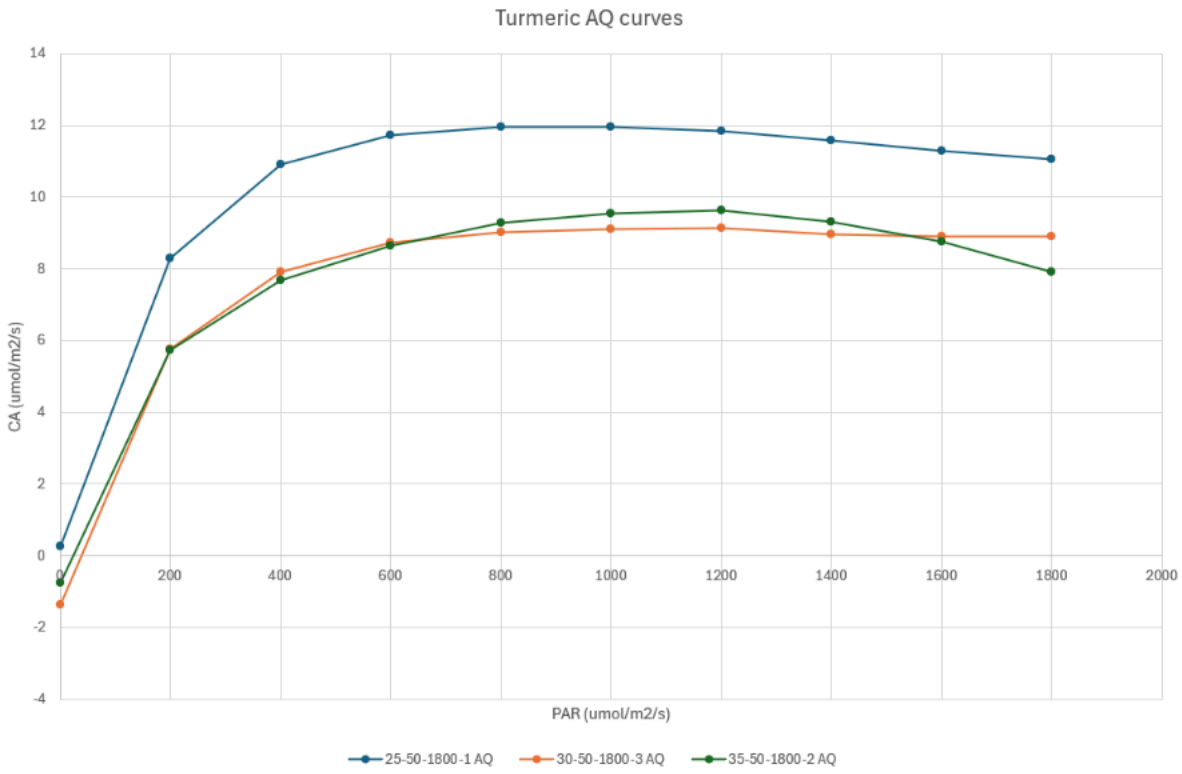

Fig.2 AQ Curves Turmeric

2.1.2 Crop 2 – Capsicum

Aci Curves – Two sets of ACI curves were analysed—one under varying temperature conditions and the other under different light levels. The results show that assimilation increases with intercellular CO_2 until saturation. However, the influence of environmental conditions is more pronounced. At around 30 °C, capsicum demonstrated the most optimal response, as both the slope and maximum assimilation rate (A) were highest at this temperature. Beyond ~1200 µmol m^{-2} s^{-1} PAR, the curves begin to saturate, confirming the photosynthetic capacity ceiling.

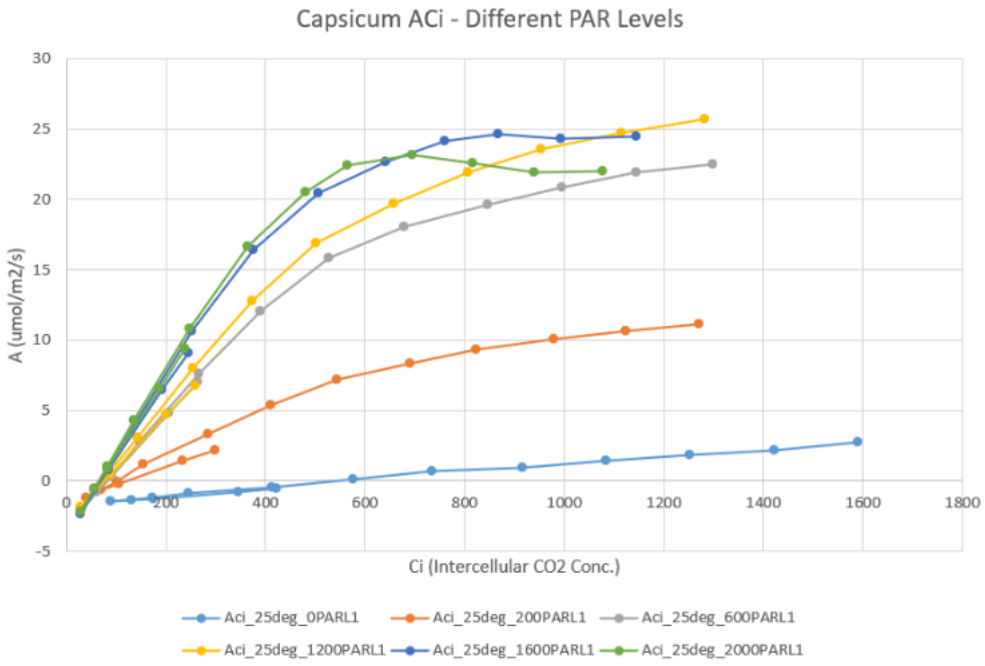

Fig.3 Aci Curves Capsicum – Diff PAR Levels

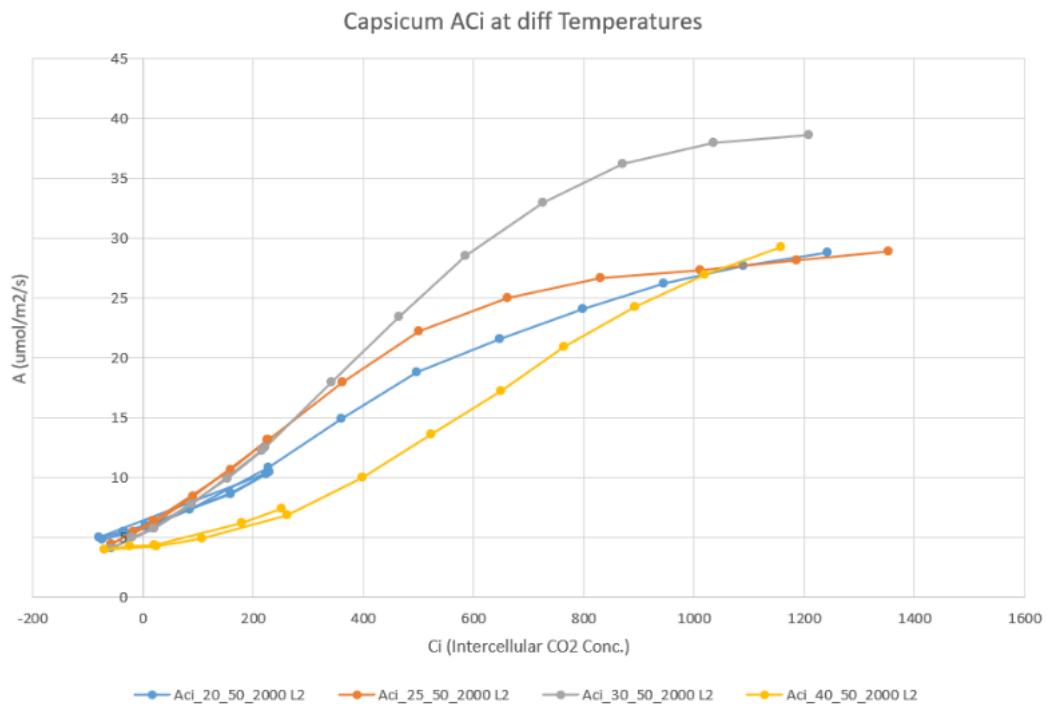

Fig.4 Aci Curves Capsicum – Diff Temperatures

AQ Curves - The light response curves for capsicum, taken at different times of the day under uniform chamber conditions, highlight the diurnal trend. From 11 am until 5 pm, very little diurnal variation is observed, suggesting that capsicum maintains relatively stable photosynthetic activity during peak daylight hours. This consistency across the day reflects capsicum's adaptation to prolonged high-light conditions.

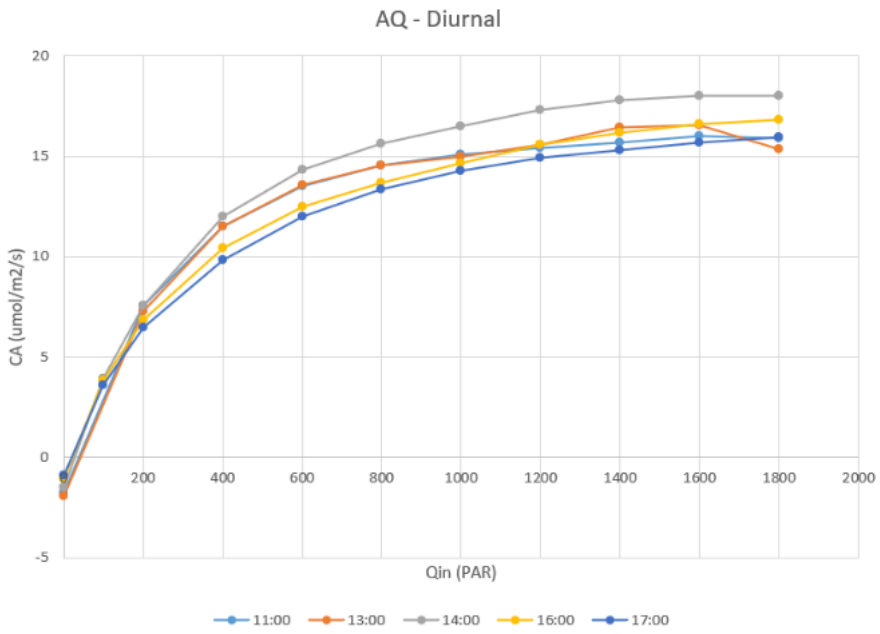

Fig.5 AQ Curves Capsicum – Diurnal

2.1.3 Crop 3 – Strawberry

Aci Curves – The Aci curve for strawberry represents the variation in photosynthetic rate with changing intercellular CO_2 concentration (Ci). From the curve, it can be inferred that the photosynthetic response is most efficient at around **25 °C**, where the assimilation rate (A) reaches its highest values compared to other temperatures.

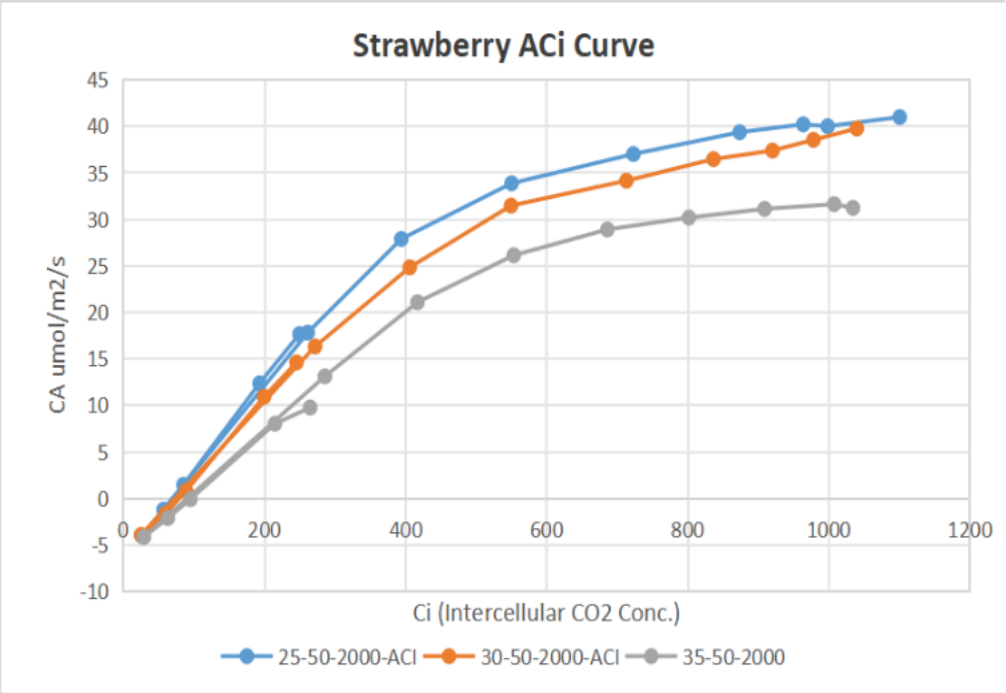

Fig.6 ACi Curves Strawberry

AQ Curves – The AQ curves illustrate the photosynthetic response of strawberry leaves to varying levels of incident PAR. From the graph, it is evident that the photosynthesis rate increases steadily with rising PAR but begins to saturate beyond approximately **600 µmol m^{-2} s^{-1}**, indicating that higher light levels beyond this point do not substantially enhance photosynthesis.

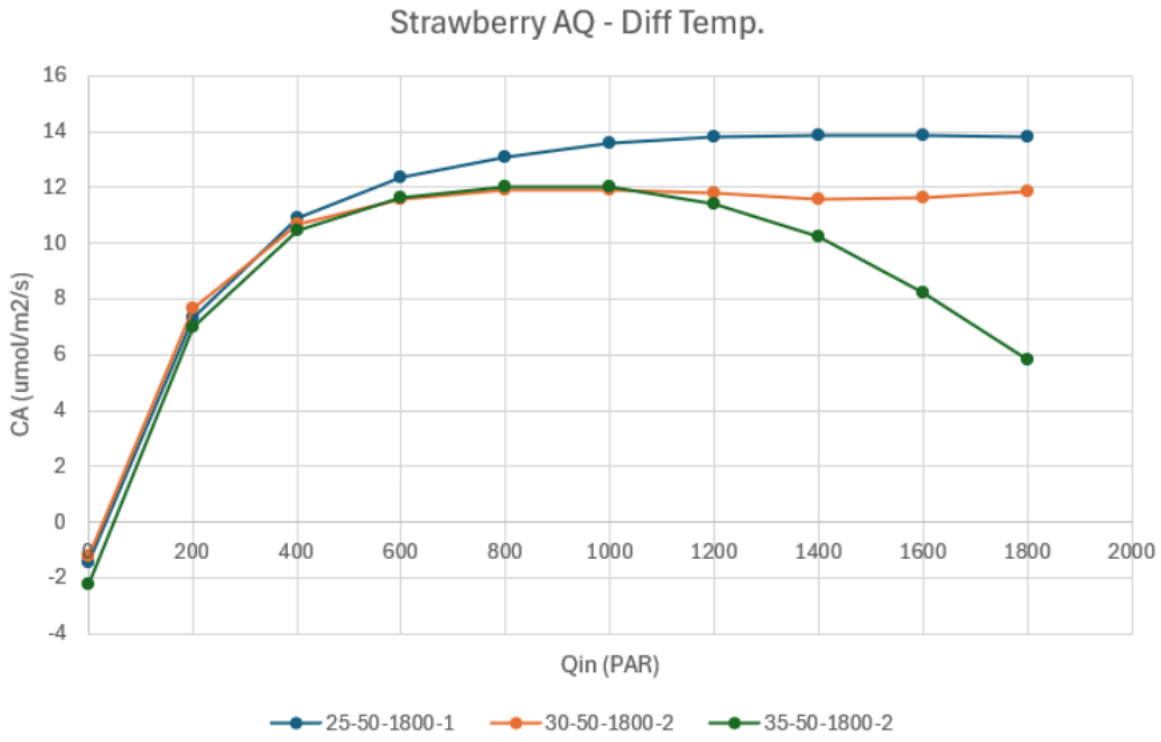

Fig.7 AQ Curves Strawberry

2.1.4 Crop 4 – Cucumber

Measurement Protocol – For cucumber, the rapid ACI automated measurement method was employed (referencing the updated measurement protocol). This approach enables faster acquisition of A–Ci response curves under varying light and temperature conditions, providing greater resolution for identifying optimal physiological responses.

Aci curves – The Aci curves below illustrate the photosynthetic response of cucumber leaves to varying intercellular CO_2 concentrations.

- In the **first set of graphs**, light intensity was varied to generate A–Ci curves at different PAR levels. It can be inferred that photosynthesis approaches saturation beyond **800 µmol m^{-2} s^{-1} PAR**, as further increases in light do not substantially raise assimilation.
- In the **second set of graphs**, temperature was varied to observe its influence on the A–Ci response. From these curves, it is evident that the optimum temperature for cucumber photosynthesis lies close to **38 °C**, where assimilation reaches its peak.

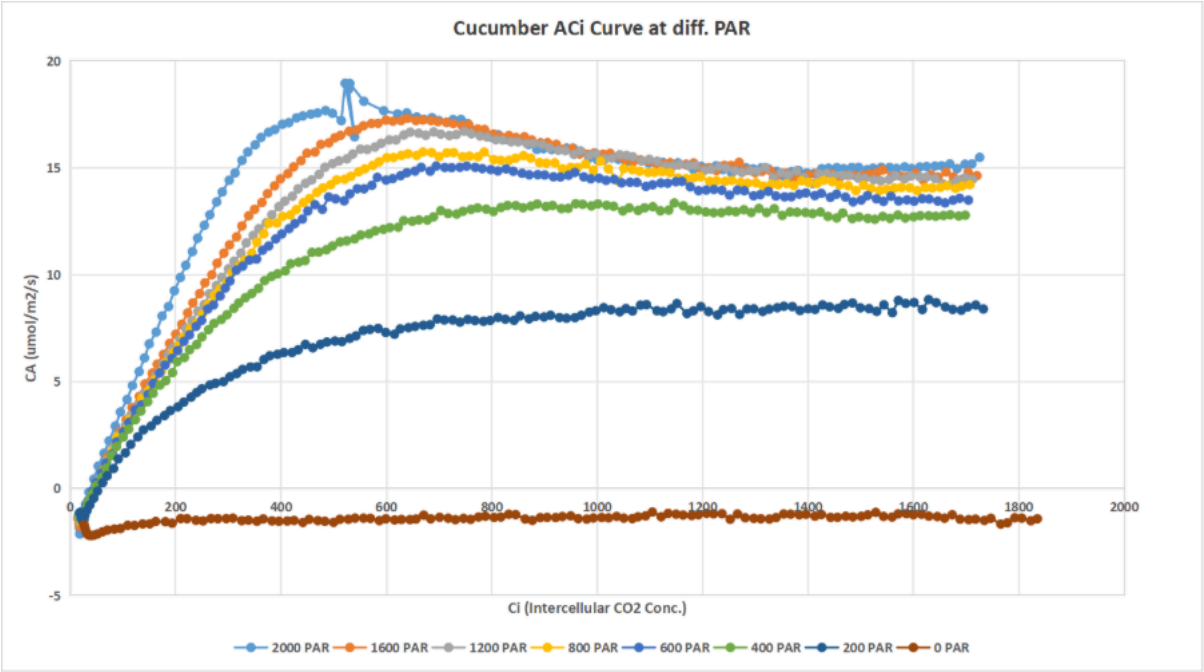

Fig.8 ACi Curves Cucumber – Diff PAR Levels

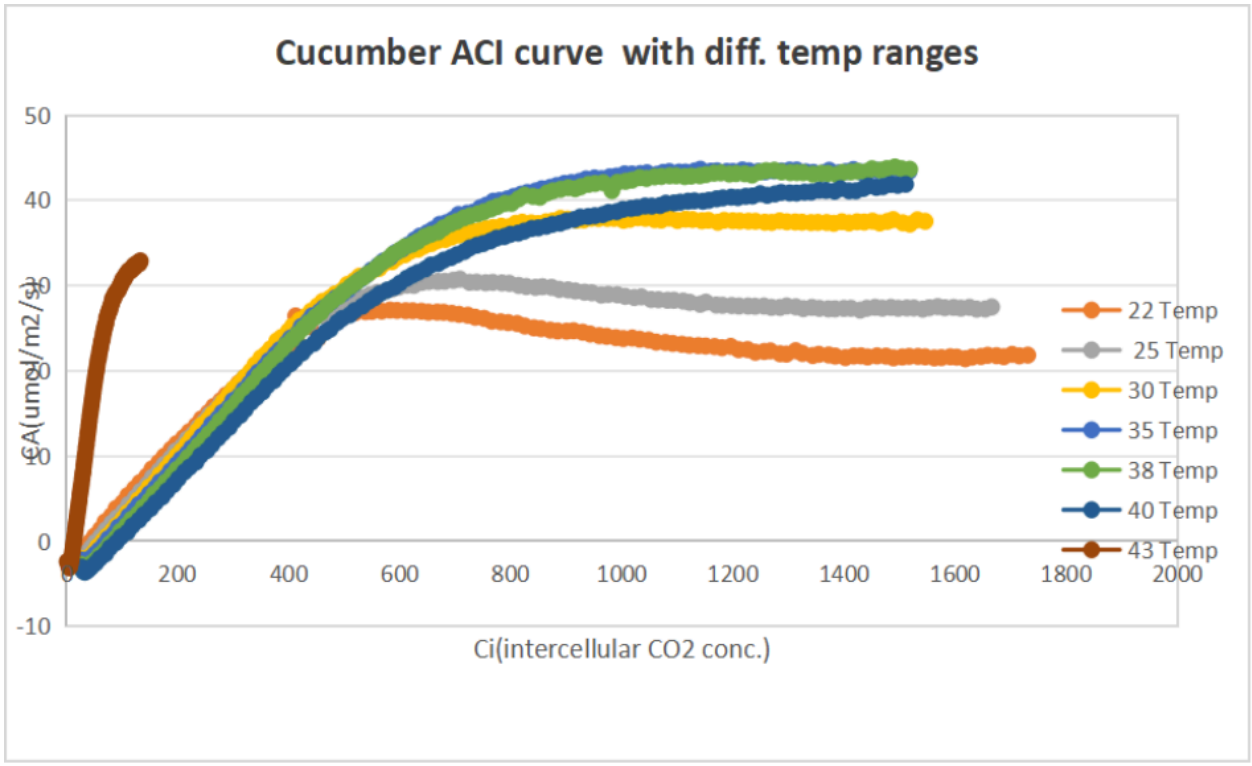

Fig.9 ACi Curves Cucumber – Different Temperatures

AQ Curves – The AQ curves demonstrate the light response of cucumber throughout the day. A clear diurnal trend is visible, with **higher photosynthetic rates in the morning** and a **gradual decline towards evening**. This drop may be attributed to cumulative stress factors such as leaf temperature rise or stomatal limitations later in the day.

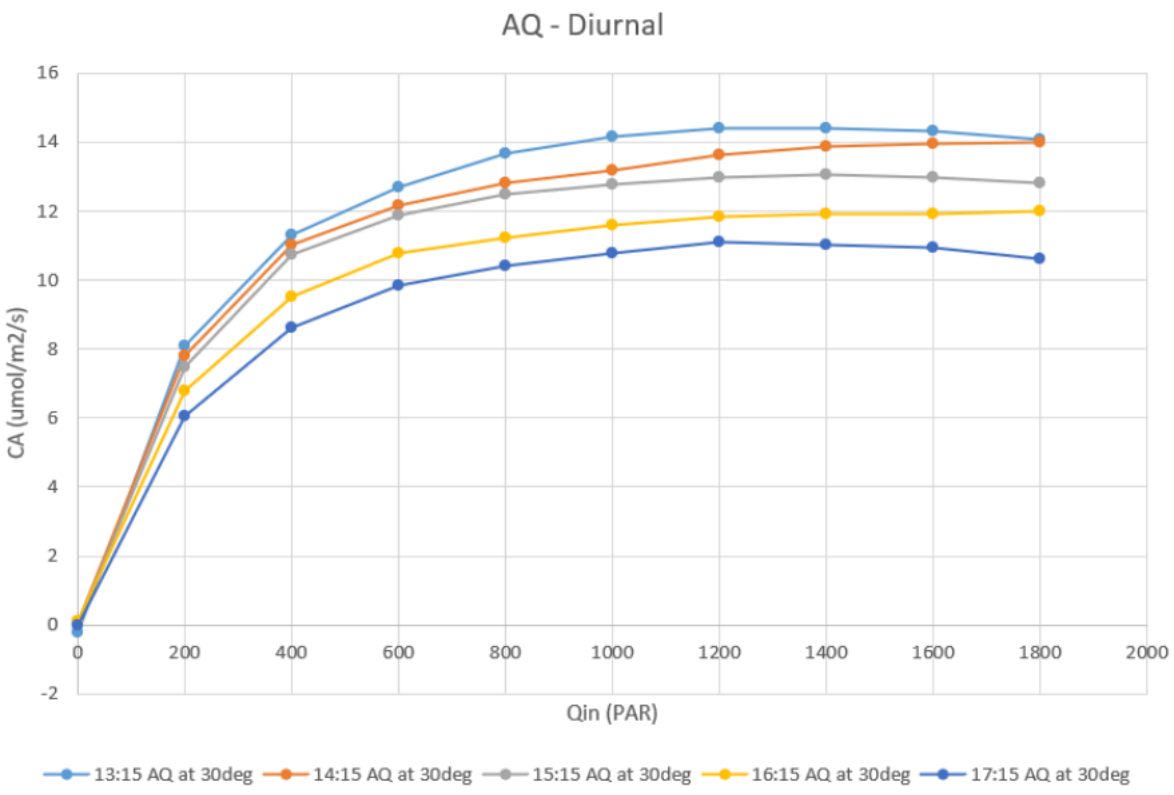

Fig.10 AQ Curves Cucumber – Diurnal Variations

2.2. PLANT ARCHITECTURE MEASUREMENTS

Helios Plant Architecture

Plant architecture refers to the three-dimensional organization of a plant's structural components — including leaves, stems, branches, flowers, and fruit — and how these elements change over time. In this project, plant architecture data are collected to serve as input for **Helios**, a plant growth and architecture modelling platform developed by the Bailey Lab. Helios uses these measurements to reconstruct virtual plants that mimic real-world structure, allowing researchers to simulate light interception, carbon assimilation, and ultimately predict biomass accumulation and yield over a full crop cycle.

The Helios plant architecture module requires a comprehensive set of parameters, such as leaf size and orientation, stem length and diameter, phyllochron (the time between successive leaf appearances), branching angles, internode length, and leaf area index. By measuring these parameters at multiple growth stages, we can capture the dynamics of plant development from **germination to senescence**. These data are crucial for accurately modelling canopy structure, understanding how environmental conditions affect plant morphology, and linking physical growth patterns with physiological processes such as photosynthesis and transpiration.

In this study, measurements were taken **manually** using tools like rulers and protractors to ensure accuracy. These values are directly mapped into the Helios architecture input format, enabling integration with the physiological parameters derived from gas-exchange analysis. When combined, this approach allows for holistic crop modelling — predicting growth patterns, light capture efficiency, and potential yield based on actual field data.

3.1] Plant Architecture Measurement – Crop Tomato

Plantation Date: 06/02/2025

I]General Plant Dimensions

Age of Measurement (Days)	Date	Height (m)	Width (m)
45	21/03/2025	0.2283	0.2516
59	04/04/2025	0.5030	0.5660
74	19/04/2025	0.6566	0.5316

II]Internode Parameters

Parameter	Units	Day 45	Day 59	Day 74
Pitch (°)	degrees	-	-	-
Phyllotactic angle (°)	degrees	90	90	90
Max vegetative buds/petiole	-	2	4	2.66
Max floral buds/petiole	-	1	4	18

III]Petiole Parameters

Parameter	Units	Day 45	Day 59	Day 74
Petioles per internode	-	1	1	1
Pitch (°)	degrees	56	56	58.33
Radius	meters	0.00152	0.00533	0.00521
Length	meters	0.0900	0.0590	0.0780

IV]Leaf Parameters

Parameter	Units	Day 45	Day 59	Day 74
Leaves per petiole	-	7	9	14
Pitch (°)	degrees	26.6	38.3	46.66
Yaw (°)	degrees	0	0	0
Roll (°)	degrees	1.33	11.6	40
Leaf length incl. petiole	meters	0.1766	0.3566	0.3566
Leaf senescence time	days	-	-	-

V]Growth Parameters

Parameter	Units	Day 45	Day 59	Day 74
Phyllochron	days/leaf	7.64	7.58	4.316
Elongation rate	m/day	0.00088	0.000751	0.000626
Vegetative bud break probability	%	43	90	83.33
Flower bud break probability	%	3	100	100
Fruit set probability	%	0	0	100
Number of fruits	-	0	0	3

VI]Phytomer Parameters

Parameter	Units	Day 45	Day 59	Day 74
Max nodes/phytomer	-	5	9	17
Internode radius initial	meters	0.00325	0.00347	0.00292
Internode radius final	meters	0.00561	0.00709	0.00829
Insertion angle tip (°)	deg/node	35	33	36.6
Internode length max	meters	0.0156	0.0650	0.0983

VII]Observed Phytomer Details

Observation No.	Length (m)	Radius (m)	Length (m)	Radius (m)	Length (m)	Radius (m)
1. (Day 45)	0.0240	0.00351	0.0333	0.00766	0.0363	0.00812
2. (Day 59)	0.0350	0.004146	0.0440	0.00753	0.0450	0.00860
3. (Day 74)	0.0366	0.00500	0.0440	0.00783	0.0463	0.00829

3.2] Plant architecture measurement – Cucumber

Plantation Date: 06/02/2025

I]General Plant Dimensions

Age of Measurement (Days)	Date	Height (m)	Width (m)
38	14/03/2025	0.1167	0.2366
55	31/03/2025	0.8766	0.695
69	14/04/2025	1.1783	0.4891

II]Internode Parameters

Parameter	Units	Day 38	Day 55	Day 69
Pitch (°)	degrees	-	-	-
Phyllotactic angle (°)	degrees	180	180	180
Max vegetative buds/petiole	-		1	1
Max floral buds/petiole	-		2	2

III]Petiole Parameters

Parameter	Units	Day 38	Day 55	Day 69
Petioles per internode	-	1	1	1
Pitch (°)	degrees	46.66	63.33	65
Radius	meters	0.0022	0.0443	0.004116
Length	meters	0.035	0.0893	0.0866

IV] Leaf Parameters

Parameter	Units	Day 38	Day 55	Day 69
Leaves per petiole	-	1	1	1
Pitch (°)	degrees	28.33	45	46.66
Yaw (°)	degrees	0	0	0
Roll (°)	degrees	0	6.66	6.66
Leaf length incl. petiole	meters	-	-	-
Leaf senescence time	days		0.1743	0.15

V]Growth Parameters

Parameter	Units	Day 38	Day 55	Day 69
Phyllochron	days/leaf	15	4.5	2.97
Elongation rate	m/day		0.0009	0.0007274
Vegetative bud break probability	%		-	-
Flower bud break probability	%	NA	0	100
Fruit set probability	%	NA	0	100
Number of fruits	-	NA	0	100

VI]Phytomer Parameters

Parameter	Units	Day 38	Day 55	Day 69
Max nodes/phytomer	-	2	12.3	25.3
nternode radius initial	neters	0.0028	0.0025	0.00300
nternode radius final	neters	0.00429	0.00765	0.00759
nsertion angle tip (°)	deg/node	20	53.3	51.66
nternode length max	neters	0.03	0.0933	0.0966

VII]Observed Phytomer Details

Observation No.	Length (m)	Radius (m)	Length (m)	Radius (m)	Length (m)	Radius (m)
. (Day 38)	).03	).002883	NA	NA	NA	NA
2. (Day 55)	).026	).00659	).0373	).00585	).05	).00512
3. (Day 69)	).0266	).006393	).03733	).005396	).05	).005163

3.3] Plant architecture measurement – Marigold

Plantation Date: 06/02/2025

I]General Plant Dimensions

Age of Measurement (Days)	Date	Height (m)	Width (m)
45	21/03/2025	).348	).2
59	)4/04/2025	).5116	).234
74	19/04/2025	).53	).226

II]Internode Parameters

Parameter	Units	Day 45	Day 59	Day 74
Pitch (°)	degrees	-	-	-
Phyllotactic angle (°)	degrees	0	0	0
Max vegetative buds/petiole	-	10	14	11
Max floral buds/petiole	-	-	9	12

III]Petiole Parameters

Parameter	Units	Day 45	Day 59	Day 74
Petioles per internode	-	2	4	2
Pitch (°)	degrees	59.3	66	75
Radius	meters	0.00224	0.00240	0.00186
Length	meters	0.0716	0.108	0.0796

IV]Leaf Parameters

Parameter	Units	Day 45	Day 59	Day 74
Leaves per petiole	-	15	16	17
Pitch (°)	degrees	16.6	31.6	35
Yaw (°)	degrees	0	0	0
Roll (°)	degrees	1.5	3.3	10
Leaf length incl. petiole	meters	-	-	-
Leaf senescence time	days	0.1183	0.0466	0.0466

V]Growth Parameters

Parameter	Units	Day 45	Day 59	Day 74
Phyllochron	days/leaf	7.5	5.21	6.059
Elongation rate	m/day	0.0007	0.00062	0.0005
Vegetative bud break probability	%	-	-	-
Flower bud break probability	%	100	100	50
Fruit set probability	%	3.3	100	100
Number of fruits	-	-		

VI]Phytomer Parameters

Parameter	Units	Day 45	Day 59	Day 74
Max nodes/phytomer	-	6	11.33	12
Internode radius initial	meters	0.00387	0.00265	0.00243
Internode radius final	meters	0.00586	0.00645	0.00626
Insertion angle tip (°)	deg/node	30	38.3	35
Internode length max	meters	0.0216	0.0566	0.523

VII]Observed Phytomer Details

Observation No.	Length (m)	Radius (m)	Length (m)	Radius (m)	Length (m)	Radius (m)
1. (Day 45)	0.0333	0.00395	0.03	0.004216	0.0338	0.00467
2. (Day 59)	0.03	0.004216	0.0333	0.00559	0.0366	0.00559
3. (Day 74)	0.0433	0.00467	0.0363	0.00554	0.0376	0.00558

3.4] Plant architecture measurement – Chilli

Plantation Date: 06/02/2025

I]General Plant Dimensions

Age of Measurement (Days)	Date	Height (m)	Width (m)
48	24/03/2025	0.137	0.228
63	3/04/2025	0.254	0.2801
78	23/04/2025	0.4483	0.353

II]Internode Parameters

Parameter	Units	Day 48	Day 63	Day 78
Pitch (°)	degrees	-	-	-
Phyllotactic angle (°)	degrees	90	90	90
Max vegetative buds/petiole	-	5	6	8
Max floral buds/petiole	-	-	13.3	14

III]Petiole Parameters

Parameter	Units	Day 48	Day 63	Day 78
Petioles per internode	-	1	2	2
Pitch (°)	degrees	68.33	73.3	79
Radius	meters	0.00168	0.00177	0.01763
Length	meters	0.0366	0.04	0.03366

IV]Leaf Parameters

Parameter	Units	Day 48	Day 63	Day 78
Leaves per petiole	-	1	1	1
Pitch (°)	degrees	6.6	26.66	28.33
Yaw (°)	degrees	0	0	0
Roll (°)	degrees	0	0	0
Leaf length incl. petiole	meters	-	-	-
Leaf senescence time	days	0.0823	0.09	0.0786

V]Growth Parameters

Parameter	Units	Day 48	Day 63	Day 78
Phyllochron	days/leaf	11.2	6.342	1.7259
Elongation rate	m/day	0.000451	0.000402	0.0003675
Vegetative bud break probability	%	-	-	
Flower bud break probability	%	0	100	100
Fruit set probability	%	0	100	100
Number of fruits	-	0	0	100

VI]Phytomer Parameters

Parameter	Units	Day 48	Day 63	Day 78
Max nodes/phytomer	-	5	7	20
Internode radius initial	meters	0.00213	0.00238	0.00208
Internode radius final	meters	0.00307	0.00378	0.00592
Insertion angle tip (°)	deg/node	31.5	53.3	48.33
Internode length max	meters	0.0142	4.466	0.0643

VII]Observed Phytomer Details

Observation No.	Length (m)	Radius (m)	Length (m)	Radius (m)	Length(m)	Radius (m)
. (Day 48)	.024	.00246	.026	.002963	.0176	.002953
. (Day 63)	.02766	.00354	.02766	.00354	.019	.0032
. (Day 78)	.02766	.00504	.02766	.00495	.0284	.00435

3.5] Plant architecture measurement – Brinjal

Plantation Date: 06/03/2025

I]General Plant Dimensions

Age of Measurement (Days)	Date	Height (m)	Width (m)
4	9/04/2025	0.2433	.3766
8	3/04/2025	0.4066	.4725
5	0/05/2025	.54	.226

II]Internode Parameters

Parameter	Units	Day 34	Day 48	Day 65
itch (°)	egrees	-	-	0
hyllotactic angle (°)	egrees	180	180	1
ax vegetative buds/petiole	-	1	1	
ax floral buds/petiole	-	-	3	3

III]Petiole Parameters

Parameter	Units	Day 34	Day 48	Day 65
etioles per internode	-	1	1	1

Pitch (°)	degrees	61.6	75	75
Radius	meters	0.00565	0.006106	0.00439
Length	meters	0.07166	0.08166	0.052

IV]Leaf Parameters

Parameter	Units	Day 34	Day 48	Day 65
Leaves per petiole	-	1	1	1
Pitch (°)	degrees	10	10	11.66
Yaw (°)	degrees	0	0	0
Roll (°)	degrees	0	0	0
Leaf length incl. petiole	meters	-	-	-
Leaf senescence time	days	0.178	0.2103	0.178

V]Growth Parameters

Parameter	Units	Day 34	Day 48	Day 65
Phyllochron	days/leaf	4.407	3.209	3.509
Elongation rate	m/day	0.1245	0.000756	0.000856
Vegetative bud break probability	%	-	-	-
Flower bud break probability	%	100	45	76.92
Fruit set probability	%	0	10	26.92
Number of fruits	-	0	0	3

VI]Phytomer Parameters

Parameter	Units	Day 34	Day 48	Day 65
Max nodes/phytomer	-	8	20.66	20.66
nternode radius initial	neters	0.005206	0.00535	0.00535
nternode radius final	neters	0.00617	0.00952	0.00952
nsertion angle tip (°)	deg/node	53.33	45	46
nternode length max	neters	0.031	0.0543	0.0543

VII]Observed Phytomer Details

Observation No.	Length (m)	Radius (m)	Length (m)	Radius (m)	Length (m)	Radius (m)
1. (Day 34)	0.022	0.007103	0.02433	0.00714	0.02766	0.006033
2. (Day 48)	0.023	0.0104	0.0213	0.01031	0.0363	0.00961
3. (Day 65)	0.023	0.01335	0.0213	0.01463	0.0363	0.01208

3.6] Plant architecture measurement – Capsicum

Plantation Date: 04/11/2024

I]General Plant Dimensions

Age of Measurement (Days)	Date	Height (m)	Width (m)
175	28/04/2025	0.79	0.4565

II]Internode Parameters

Parameter	Units	Day 175
Pitch (°)	degrees	-
Phyllotactic angle (°)	degrees	180
Max vegetative buds/petiole	-	38
Max floral buds/petiole	-	16

III]Petiole Parameters

Parameter	Units	Day 175
Petioles per internode	-	3-4
Pitch (°)	degrees	65
Radius	meters	0.00297
Length	meters	0.052

IV]Leaf Parameters

Parameter	Units	Day 175
Leaves per petiole	-	1
Pitch (°)	degrees	10
Yaw (°)	degrees	0
Roll (°)	degrees	0
Leaf length incl. petiole	meters	-
Leaf senescence time	days	0.12

V]Growth Parameters

Parameter	Units	Day 175
Phyllochron	days/leaf	4.069
Elongation rate	m/day	0.00024
Vegetative bud break probability	%	-
Flower bud break probability	%	100
Fruit set probability	%	100
Number of fruits	-	100

VI]Phytomer Parameters

Parameter	Units	Day 175
Max nodes/phytomer	-	41
Internode radius initial	meters	0.00381
Internode radius final	meters	0.0104
Insertion angle tip (°)	deg/node	45
Internode length max	meters	0.086

VII]Observed Phytomer Details

Observation No.	Length (m)	Radius (m)	Length (m)	Radius (m)	Length(m)	Radius (m)
. (Day 175)	0.05	0.00625	0.055	0.006223	0.042	0.00621

Images while collecting data:


DOMS
GEOFINE

2.3 Fogging Efficiencies and Microclimate Measurements

Climatic conditions relevant to protected cultivation can broadly be classified into four subgroups:

1. **High temperature (> 35 °C) and high humidity (> 60% RH)**
2. **High temperature (> 35 °C) and low humidity (< 30% RH)**
3. **Low temperature (< 20 °C) and high humidity (> 60% RH)**
4. **Low temperature (< 20 °C) and low humidity (< 30% RH)**

Among the various strategies for microclimate regulation, **evaporative cooling** is an age-old and well-established technique. However, its effectiveness is restricted primarily to conditions of **high temperature (> 35 °C) combined with low humidity (< 30% RH)**. Under such conditions, the evaporation of water from wetted surfaces (as in fan–pad systems) or from atomized droplets (as in foggers) absorbs significant quantities of heat in the form of **latent heat of vaporization**. This results in a measurable reduction in air temperature while simultaneously raising the humidity level inside the polyhouse.

The increase in both **absolute humidity (specific humidity)** and **relative humidity** within the growing environment enhances plant physiological responses. In particular, it promotes **stomatal opening**, which facilitates faster **gaseous exchange**—primarily the uptake of carbon dioxide (CO_2) and the release of oxygen (O_2). This optimized stomatal activity directly contributes to improved photosynthetic performance and, consequently, better crop growth and productivity in controlled environments.

Methodology

Choice of Site: Study was carried out at Pabal, a village in Pune district of Maharashtra, as a site for creating infrastructure for data collection on the energy balance model and fogger efficiency testing. Pabal village experiences hot and dry climates with an annual rainfall of approximately 470mm, categorizing it within semi-arid zone. This limited precipitation presents

challenges for open-field agriculture, making it a relevant location to assess how polyhouse structures can mitigate water scarcity and enhance crop productivity.

Infrastructure: For this study, a polyhouse structure was constructed with dimensions of **9 m in length, 4 m in breadth, and 4.75 m in height**. Higher surface is of polyhouse boundaries could be achieved by increasing height of structure. Tall poly house will in turn generate higher air resistance and lower structural stability. A sweet spot of above mentioned dimension was hence chosen. This geometry can sustain wind up to 120 km/h, of volume 156m^3 and 35m^2 surface area exposed to fogging and solar radiations.

- The structure was made using a **Galvanized Iron (GI) pipe for the frame**, with **single-layer LDPE polysheet** (poly film UV stabilized 200 micron) of total size approx. 170 m^2 used for both the roof and the walls.
- The meteorological parameters used for the study reflect peak summer climatic conditions typical of the region (18.828800,74.046417). These include a **maximum solar irradiance of approximately 1000 W/m²**, a **maximum ambient temperature of 40°C with 20% relative humidity.** The minimum temperature which could be achieved is wet bulb temperature under given atmospheric conditions. How ever for practical purpose we have assume **minimum achievable temperature at 85% relative humidity.** These values are critical for psychrometric calculations, as they help

determine the evaporative cooling potential of the fogging system under both dry and humid conditions.

Measurement:

From earlier studies and our own experience, it is known that only about 20% of the water released by foggers is used for evaporative cooling. The rest, in the absence of plantation, falls onto the soil surface. This wetting of soil changes the heating and cooling pattern inside the polyhouse. To avoid this effect, the floor was covered with a black HDPE plastic sheet. The black color was chosen deliberately because it simulates the behavior of wet black cotton soil, which can absorb up to 98% of the visible and infrared spectrum. On top of this sheet, polyester blankets were spread to absorb the water falling on the ground. By measuring the weight difference of the blankets before

and after each experiment, we were able to calculate the amount of water that settled on the floor instead of being evaporated. This portion of water, although not directly used for cooling, still contributed to raising the relative humidity inside the polyhouse. In this way, the setup helped us more accurately assess the efficiency of fogging water utilization for cooling and humidity enhancement.

- The fogging system was tested using three different types of foggers, each with a unique discharge rate. Fogger technical specifications are given below separately.
- Temperature and humidity data collected with automated data loggers, while air flow readings taken by a hand-held Fluke's anemometer.

Fig.1 Polyhouse structure

Energy Balance Modelling for Protected Cultivation Scenarios

In this section, we create energy balance equations to predict temperature and humidity inside closed or controlled systems given a certain external climate and irradiation, whose outputs are compared with what was observed in our sample microclimate facility, for basic validation.

Below I have share the documentation of 1 st discussion on heat measurement. This is basically theoritical ideas of how heat is transferred in polyhouse and get trapped increasing the temperature inside.

https://docs.google.com/document/d/1DvMgFhyFP-KS0qgh2gTQa8xHVdIjATL6/edit?usp=sharing&ouid=116983018007863026538&rtpof=true&sd=true

2th discussion on heat measurement

https://docs.google.com/document/d/193rM42EQdbcVknkQ8DvnbT2ZGggW38E1/edit?usp=sharing&ouid=116983018007863026538&rtpof=true&sd=true

3 rd discussion on heat measurement. This calculation is done by recording actual temperature over a period of time

https://docs.google.com/document/d/1L_6Rq_m09UVAdQYzcQN-8GsNlrZOqqLy/edit?usp=sharing&ouid=116983018007863026538&rtpof=true&sd=true

Finding the maximum potential for evaporative cooling in a closed system:

To evaluate the maximum possible cooling effect of an evaporative system inside a closed polyhouse, the psychrometric parameters of the internal air were analyzed under peak summer conditions.

Initially, it was observed that the maximum temperature in a fully enclosed polyhouse reached 65°C with a relative humidity of 8 %. Based on these conditions, the maximum evaporative

cooling potential is calculated below by using psychrometric principles related to wet bulb temperature (WBT) and dry bulb temperature (DBT).

T= 65°C, RH= 8%

WBT = 30.08°C

Wet-Bulb Depression: The difference between DBT and WBT. A larger depression indicates greater potential for evaporative cooling.

WBD = 65°C- 30.08°C = 34.92°C

However, in practice, evaporative cooling systems do not achieve 100% of this theoretical potential. Their performance depends on design, water quality, airflow rate, and distribution efficiency. For practical estimation, an **evaporative cooling efficiency of 80%** is considered. The actual achievable cooling is therefore:

Considering the cooling efficiency of evaporative efficiency - 80%

Maximum evaporative cooling temperature = efficiency * WBD

= 0.8 * 34.92

= 27.98°C ~ 28°C

So, the maximum evaporative cooling potential for an enclosed system at the highest maximum temperature (65°C) is approximately 28°C reaching to 80% RH .

This analysis highlights that during extreme summer conditions (65 °C, 8% RH), evaporative cooling has a very high potential due to the large wet-bulb depression (34.92 °C). At 80% system efficiency, the maximum achievable cooling is about 28 °C. This demonstrates the importance and effectiveness of evaporative cooling systems in polyhouses located in arid and semi-arid climates where relative humidity is low.

The experiment was carried on 25th April 2025, the inside temperature of polyhouse was noted be 65°C. As planned the system was close with curtain down and pads covered with polyethylene sheet. The only fogger available at site was 4-way fogger, procured from Jain Irrigation. We have noted temperature coming down from 65°C to 45°C with humidity 80% in 15 min. with discharge of water 103 lit. continuation discharge not resulted in further cooling

outside temperature was 38°C. higher poly-house temperature during continuous water discharged form foggers puzzled us. Analysing the situation, we came to conclusion that fogging area i.e . A microclimate zone must have been reached to 100% RH, resulting into zero evaporation and hence further cooling.

Below is the link provided which includes data of above experiment performed:
https://docs.google.com//d/1FpXWr2WNtQqsqzF_SLzNfRPrkw39sEEY/edit?usp=sharing&ouid=116983018007863026538&rtpof=true&sd=true
To overcome the formation of a saturated microclimate zone, **air turbulence was introduced** by operating a fan with an airflow capacity of **15,000 CFM**. This intervention enabled further evaporation, and consequently, the polyhouse temperature decreased to **29 °C**.Since all four foggers were not available on-site, we could not test the complete setup as originally planned. However, an additional set of observations was recorded: after activating **internal air circulation**, the temperature dropped from **60.32 °C with RH 14% to 29 °C with RH 67% within 30 minutes**.

Please find the data below:

https://docs.google.com/spreadsheets/d/1mmOM4D2imq9SuQ_DSm1qS9--4F0_utlO/edit?usp=sharing&ouid=116983018007863026538&rtpof=true&sd=true

Installing Temperature and Relative humidity sensor

For continuous monitoring of environmental conditions, **temperature and humidity sensors were installed through automated data loggers**. These data loggers record and upload measurements to a **web-based channel created using Firebase projects**, ensuring real-time accessibility of data.

The sensors integrated in the system included:

- **HDC1080** for temperature and humidity measurement
- **VEML7700** for ambient light (lux) sensing

The use of **automated data loggers** is crucial for this project, as they provide:

1. **Accurate and time-stamped data collection** without manual intervention.

2. **Continuous monitoring**, which helps capture dynamic changes in polyhouse microclimate conditions.
3. **Data accessibility and storage on cloud platforms**, enabling remote tracking and long-term analysis.
4. **Objective evaluation of system performance**, such as cooling efficiency of foggers and effectiveness of air circulation.

Thus, data loggers form the **backbone of experimentation and analysis** in this study, allowing scientific validation of the observed cooling phenomena and supporting optimization of the fogging system.

The positions of data loggers are shown in the diagram below-

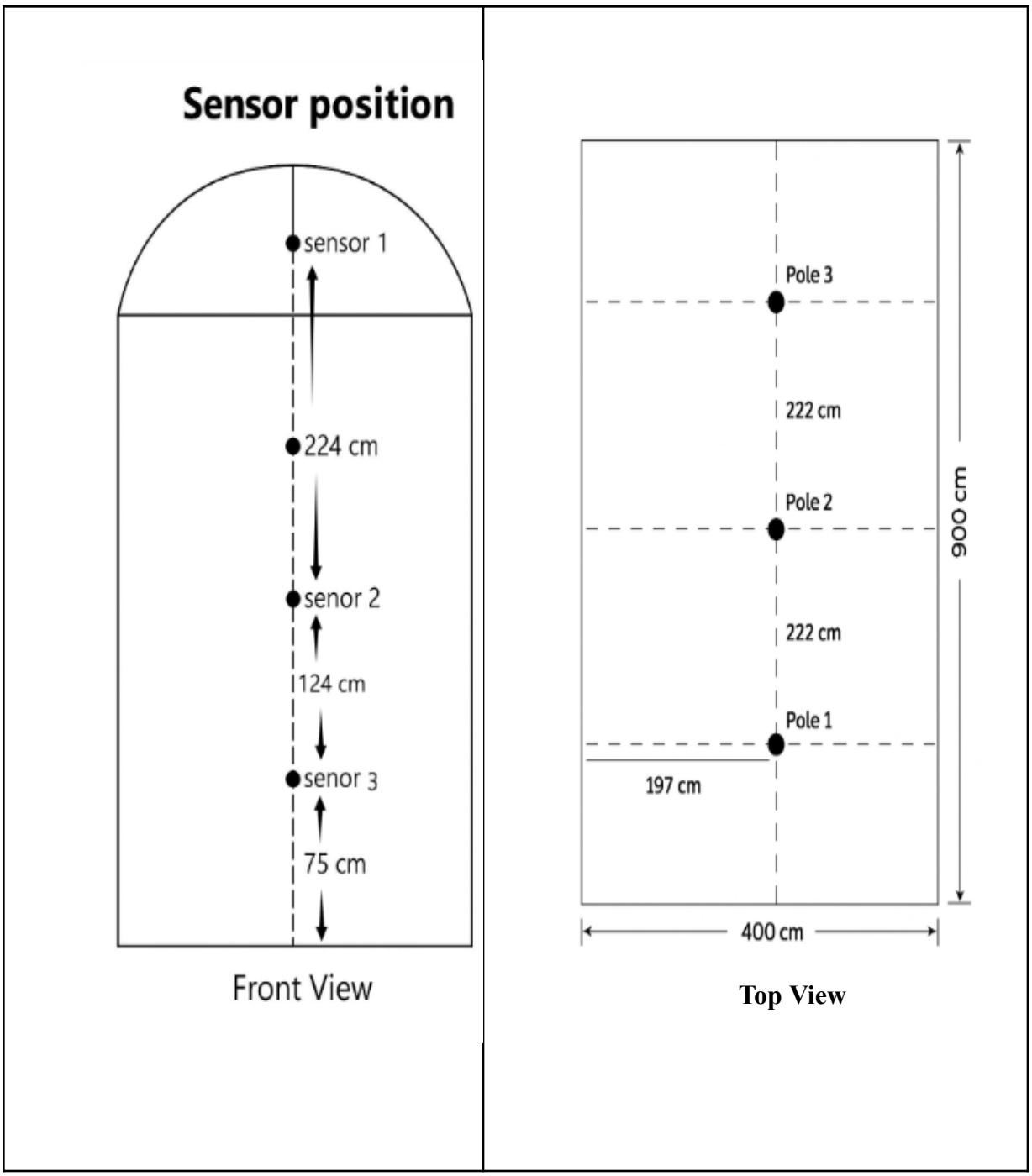

Fig.2 Schematic representation of positioning of data loggers

Fig.3 While making connections in data loggers

3] Mapping a fogger efficiency for an evaporative cooling system:

All three foggers *viz.* 4-way fogger, Super fogger, Netafim fogger are tested for their evaporative cooling efficiency. For this, an experimental setup was created with data collection on temperature & humidity rise & fall, water use, and air exchange rate. An energy balance equation was created for a collected data set and compared with theoretical values. Following are the details of the experiment & results:

Fan Pad System Design:

Finding the optimum airflow for evaporative cooling:

The basic requirement of a system at equilibrium is input should be equal to outgo. In case of polyhouse temperature equilibration. In coming energy which is mainly solar irradiation should be matched with cooling equipment.

- We decide to theoretically calculate new inflow of energy in case of polyhouse. We decide to choose the worst possible scenario. Hottest temperature of year and highest wind flow. The calculated value was 12.8 kJ/s under 1000 W/m² solar irradiance. The assumption mead 85% transparency for visible spectra 10 % for far IR and 25 % for near IR. We then decided to check our assumption before designing exhaust fan wind flow.

The required airflow to maintain optimal temperature conditions (maximum temp 35°C) in a polyhouse, a set of experiments was conducted in the polyhouse tunnel. Based on the data collection on heat gain, the exhaust fan discharge in Cubic Feet Per Minute (CFM) is decided.

Experimental setup:

Initially evaporative cooling data was collected in a close system. It involved recording temperature drop with water fogging, internal air circulation with a exhaust fan of 3 HP motor with flow rate of 15,000 CFM and then further opening of side curtains. Data on temperature drop & humidity gain was recorded.

The polyhouse water fogging was stopped, curtains were lowered. Inside soil was covered with polyethylene sheet to avoid evaporation of soil moisture gained during fogging and hence cooling during heat gain regime. Poly-house temperature was allowed to raised due to solar irradiation up to 35°C The data loggers recorded, temperature and humidity and heat gain was calculated to determine the required airflow rate (CFM).

Steps involved in data collection-

1. Cooling Phase: The Polyhouse temperature was reduced using foggers, fans, and side vents.

2. After getting the temperature reduced, the foggers and fan were deactivated, and vents were closed.
3. The soil surface was covered with an HDPE sheet to avoid unaccounted head gain or loss.
4. Temperature rise measurement: Temperature increase was recorded until reaching 35°C.
5. Heat gain calculation: The Total heat gain was calculated based on temperature rise data.
6. CFM determination: The Required CFM was determined based on calculated heat gain.

Data link- https://docs.google.com/spreadsheets/d/1mmOM4D2imq9SuQ_DSm1qS9--4F0_utlO/edit?usp=sharing&ouid=116983018007863026538&rtpof=true&sd=true

Result:

- The experiment yielded a heat gain of 2.99 kJ/s on a sunny day, which was lower than the calculated value of 12.8 kJ/s under 1000 W/m² solar irradiance.
- To remove this 2.99 kj/s of heat, the air flow required is calculated as follows-

$Q = m*cp*\Delta T$

Q = heat trapped in kj/s = 2.99 KJ/s

Cp = specific heat capacity of air = 1.005 KJ/s

ΔT = (outer air temperature - internal air temp) = (30 - 27.5) = 2.5

m = mass of air

2.99 = m x 1.005 x 2.5

m= 2.99 kg/ 2.51 kg per m^3

m= 1.19 m^3/s

Air flow = 1.19 m^3 / 5.5 m^2 = 0.21 m/s

m = 1.19 m^3/s (2521.46 CFM)

Based on the heat gain values, the corresponding CFM requirements were:

- Approx. 8000 CFM for 12.8 kJ/s heat gain (theoretical calculative value)

- Approx. 2000 CFM for 2.99 kJ/s heat gain (experimental value)

Considering these values, it was decided to install fans with a CFM rating of 4000 (8 fans @ 500 CFM), which is approximately half of 8000 CFM (calculative value) and double of 2000 CFM (practical value).

Exhaust fan positioning:

The genesis for fan positions is as follow-

- The air flow needs to be even & distributed (avoiding pocketing).
- They should be energy efficient.
- Able to control (manipulate) air flow rate (with energy regulators).

Based on the above considerations, 8 exhaust fans (500 CFM) were installed at staggered positions.

For better understanding effects of single large fans vs multiple small fans, refer to below schematic diagram of same.

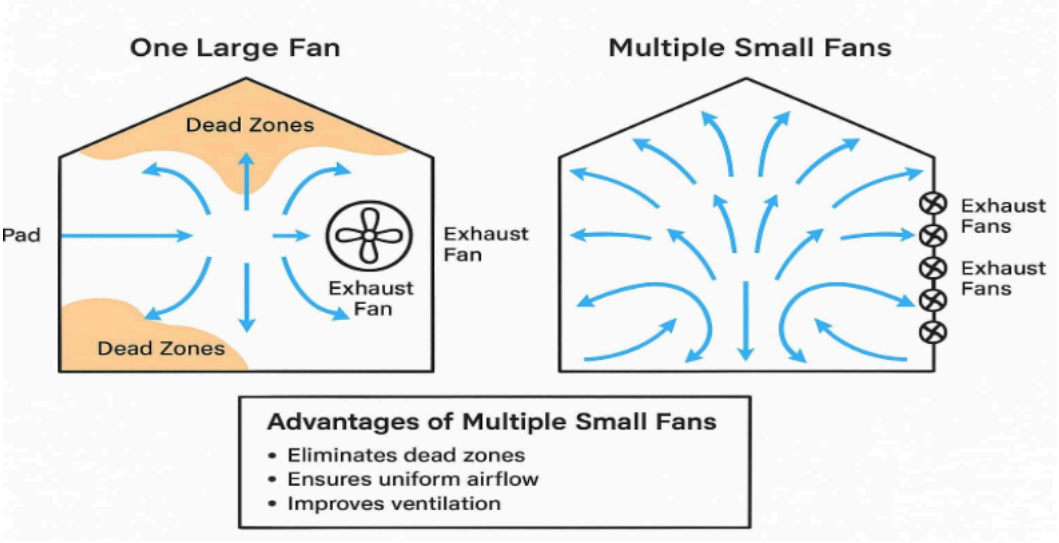

Fig. Conceptual schematic representation to compare the betterment of a single large fan vs multiple small fans

Fan position layout-

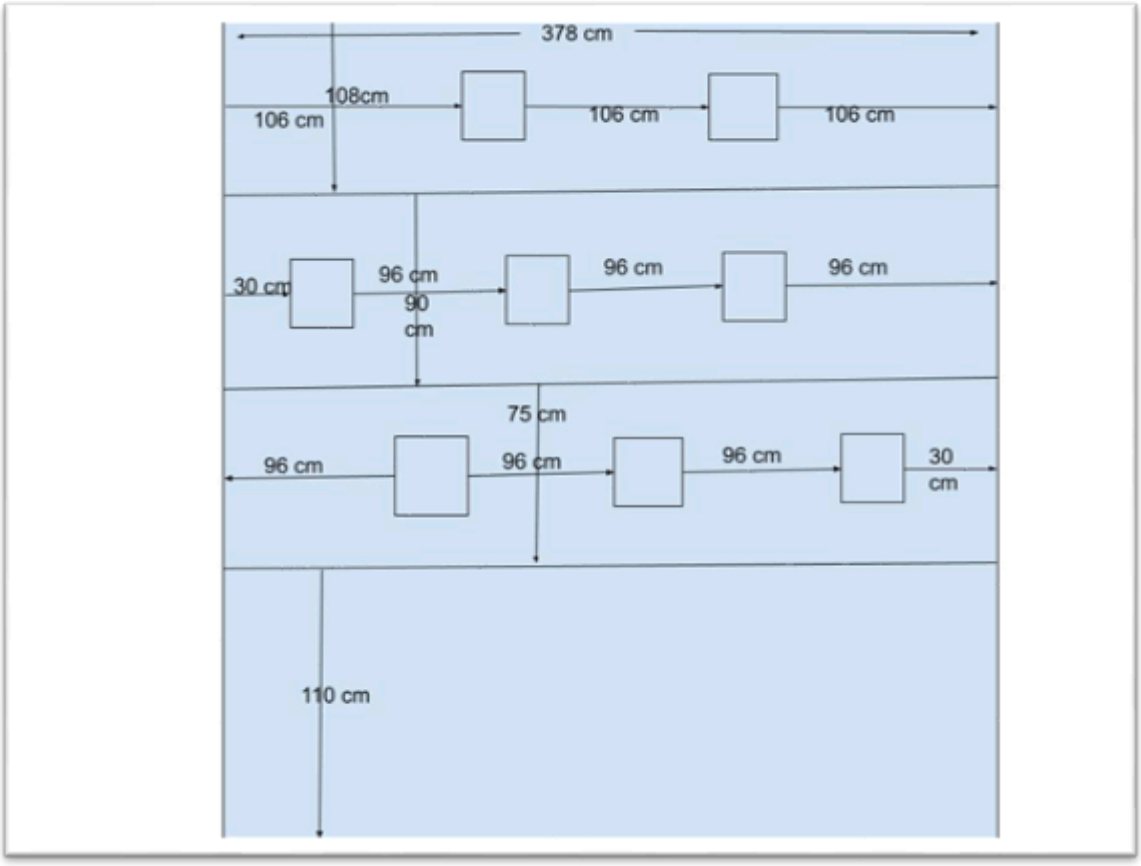

Fig. Layout figure for positioning of fans

In above figure fan 1 and fan 2 are installed in the upper section to remove heat accumulated in the hemisphere. Fan 3,4,5,6,7,8 are installed on a wall in staggered mode just opposite to the cooling pads, aligned at the same height as the cooling pads, to ensure removal of humid air from all zones within.

2.3.2 Testing fogger cooling rate

All three fogger viz. Jain 4-way fogger, Super fogger (green), Netafim Cool net Pro 4-way (light green), were tested individually on a system.

Measuring flow rate of fogger

- To determine the actual discharge rate of the foggers, a simple collection method was employed. Each fogger unit consisted of four nozzles. A single plastic bottle was securely tied to the outlet of the fogger so that water from all four nozzles was collected together.
- The fogger was operated at the recommended working pressure for a fixed interval of **30 seconds**. The quantity of water collected in the bottle during this period was measured using a graduated cylinder. The discharge volume was then extrapolated to an **hourly flow rate (litres per hour, LPH)** using the formula:

Flow rate (LPH)= { Collected volume (litres)/ Time (seconds) }×3600

- This procedure enabled the determination of the **experimental flow rate** of the foggers, which was then compared with the **stated manufacturer's flow rate** to evaluate accuracy and performance.
- Flow rate of all three fogger were measured using the same procedure.

Observation table no.1 : Measuring flow rate of foggers

r. No.	ogger type	roplet size in nicrons	perating ressure(kg/cm^ ²)	tated flow rate LPH)	xperimental low rate (LPH)
.	lain 4-way Fogger	90	4	28	24
.	uper fogger (green)	69	3-3.5	21	19
.	Netafim Cool net Pro -way (light green)	65	4	22.4	20

Note-

- Make of foggers - https://www.jains.com/PDF/Catalogue/Sprinkler/Fogger.pdf
- Make of Super foggers- https://www.jains.com/PDF/Catalogue/Sprinkler/Super%20Fogger.pdf

- Make of Netafim foggers- https://www.netafim.com.au/bynder/2F4F46C9-C2FF-49EB-8831352BCD927D8F-netafim-coolnet-pro-product-sheet.pdf
- These discharge rates are essential to understanding how much water is introduced into the air for evaporative cooling and help estimate the latent heat absorbed during fogging.
- For the experiment, the foggers were mounted on a **black polyethylene (PE) lateral tube of 18 mm diameter**. The length of the lateral tube was **9 m**, and foggers were installed at **1 m spacing** along the tube. In this arrangement, a total of **9 foggers** were fixed on the lateral. The lateral was suspended such that the foggers were positioned at a uniform height of **3.5 m above the ground level**, ensuring proper distribution of fine mist within the experimental area.
- A **3 HP** submersible-type pump installed for foggers with a 4 kg/cm2 pressure rating.
- Each fogger type was tested individually for discharge rate and evaporative cooling efficiency.

Conclusion:

- The experimental testing method successfully quantified the actual discharge of foggers under working conditions.
- All foggers delivered **slightly less water** than the rated flow, highlighting the importance of field testing instead of relying only on manufacturer specifications.
- Among the tested models, **Jain fogger supplied the highest water volume**, but its larger droplet size may reduce evaporative cooling efficiency.
- **Netafim Cool Net Pro fogger** achieved a balanced performance, with discharge close to rated values and smaller droplet size, making it more suitable for cooling applications.
- For applications like greenhouse cooling, foggers with **smaller droplets and consistent discharge (e.g., Netafim, Super fogger)** may perform better than those with higher but coarser discharge.

2.3.3 Measuring Cooling Rate of Foggers

To evaluate the cooling performance of different fogger types, experiments were conducted inside a polyhouse maintained in a controlled setup.

1. **Polyhouse Preparation:**
    a. The polyhouse was kept completely covered from all four sides to minimize external air exchange.
    b. Foggers were installed at a uniform height of 3.5 m from the ground, mounted on an 18 mm black polytube.
    c. A total of 9 foggers of each type were installed at 1 m spacing along a 9 m length of the polytube.
2. **Pre-conditioning for Experiment:**
    a. The experiment was carried out when the ambient humidity was around 62%-64%, but there was sunlight outside.
    b. To ensure realistic cooling demand, readings were taken only after the internal humidity of the polyhouse dropped to around **45%**, accompanied by an increase in temperature.
    c. This condition simulated the hot and dry microclimate inside the polyhouse, suitable for testing fogger cooling efficiency rate.
3. **Fogger Operation:**
    a. Each fogger type was tested separately.
    b. The foggers were operated for a fixed duration of **14 minutes**.
    c. Temperature and humidity readings were recorded at the start and at the end of the operation to determine the **temperature drop (ΔT)** and corresponding cooling rate (°C/min).
4. **Experimental Design for Repeatability:**
    a. To avoid interference from residual soil moisture, only one fogger type was tested per session.
    b. For the **first fogger type**, data was collected on 1st August,2025.
    c. For the remaining two fogger types, experiments were conducted on 3rd August,2025 **in two different sessions (morning and afternoon).**

d. This ensured that the soil surface had adequate time to dry between tests, preventing excess humidity or wet soil conditions from affecting subsequent results.

5. **Data Collection:**
    a. Along with temperature drop, the **water consumption** of each fogger type was calculated based on its measured experimental flow rate (LPH).
    b. Efficiency was evaluated in terms of **temperature drop per litre of water used**.

Below is the link given to the data recorded :

https://docs.google.com/spreadsheets/d/1smMN4ydnMv1uE-2fQ2YMJMQPEqKrysBZ1knbImDUUc4/edit?usp=drivesdk

Observation table no. 2: Measuring cooling rate of foggers

r. No.	ogger type	emp drop °C)/ 14 mins	rop rate (°C)/ min	Vater used according o experimental flow ate of fogger(litres/14 nins)	xperimental flow ate (LPH) of each ogger
.	Jain 4-way Fogger (9 os.)	1.8	0.129	50.4	24
.	Super fogger green) (9 nos.)	5.52	0.394	44.1	. 9
.	Netafim Cool net Pro -way (light green)(9 os.)	5.56	0.397	46.6	20

Observations (from Table No. 2)

1. The **Super fogger** and **Netafim Cool Net Pro fogger** achieved significantly higher temperature drops (≈5.5 °C in 14 minutes) compared to the **Jain 4-way fogger**, which achieved only 1.8 °C under similar operating conditions.

2. The **cooling rate per minute** was nearly **three times higher** for the Super and Netafim foggers (≈0.395 °C/min) than for the Jain fogger (0.129 °C/min).
3. Water usage during 14 minutes was highest for the **Jain fogger** (50.4 L) and slightly lower for **Super (44.1 L)** and **Netafim (46.6 L)**, despite their much higher cooling effect.
4. This indicates that **Jain fogger consumed more water but provided less cooling**, while **Super and Netafim foggers provided maximum cooling with comparatively lower water usage**.
5. Between Super and Netafim, the performance was almost equal in terms of cooling rate, but Netafim had a marginally higher cooling (5.56 °C vs. 5.52 °C) with slightly more water.

Conclusions

- The cooling efficiency of foggers strongly depends on the balance between droplet size and flow rate. Smaller droplets (as in Super and Netafim foggers) enhance evaporation and cooling.
- The Jain 4-way fogger is less efficient for cooling applications, as it consumed ~15% more water but achieved only ~⅓ of the cooling compared to the other foggers.
- The Super fogger showed the best water-use efficiency, producing a 5.52 °C temperature drop with the least water consumption (44.1 L).
- The Netafim Cool Net Pro fogger performed nearly equal to Super, with a slightly higher cooling effect but at the cost of ~2.5 L more water.
- Overall, Super fogger is the most efficient choice for cooling (higher °C drop per litre of water), while Netafim fogger is also a close second, both being far superior to the Jain fogger.

2.4 Fogger choking experiment by using $CaSO_4$ (Calcium Sulphate) for studying permanent hardness

Fogger nozzles get choked due to the presence of salts like magnesium, calcium, sulphates, chlorides, bicarbonates in water . In this experiment the choking behaviour is observed in actual field conditions. So, that we can set cleaning methods through different ways.

Choking foggers by $CaSO_4$ represents permanent hardness caused by calcium and sulphates. This salts does not fully dissolve in water as it has very low solubility compared to other salts present in water, even if water is boiled the hardness remains, so for this reason we chosed $CaSO_4$ for efficient choking of foggers.

Preparation of $CaSO_4$ solution : $CaSO_4$ Concentration (ppm) = 2100 ppm = 2.1 gm/litre (for quick choking of foggers selected highest concentration of $CaSO_4$)

For 700 litres of RO water = 0.0021 kg x 700 litres = 1.47 kg of $CaSO_4$.

Why RO water and not normal water was used : RO water is used for experiment cause RO water has low TDS, that means it does not contain salts like calcium, sulphates, chlorides, magnesium, bicarbonates. This makes it a controlled, clean baseline - so when $CaSO_4$ is added, almost how much mineral content is present is known. Whereas, normal water already has unknown and variable amounts of hardness salts.

RO water qualities -

pH - 5.98 EC - 24 us/cm TDS - 12 ppm

RO + $CaSO_4$ water qualities -

pH - 6.81 EC - 1445 us/cm TDS - 722 ppm

This hike in EC and TDS ensures blockage of foggers.

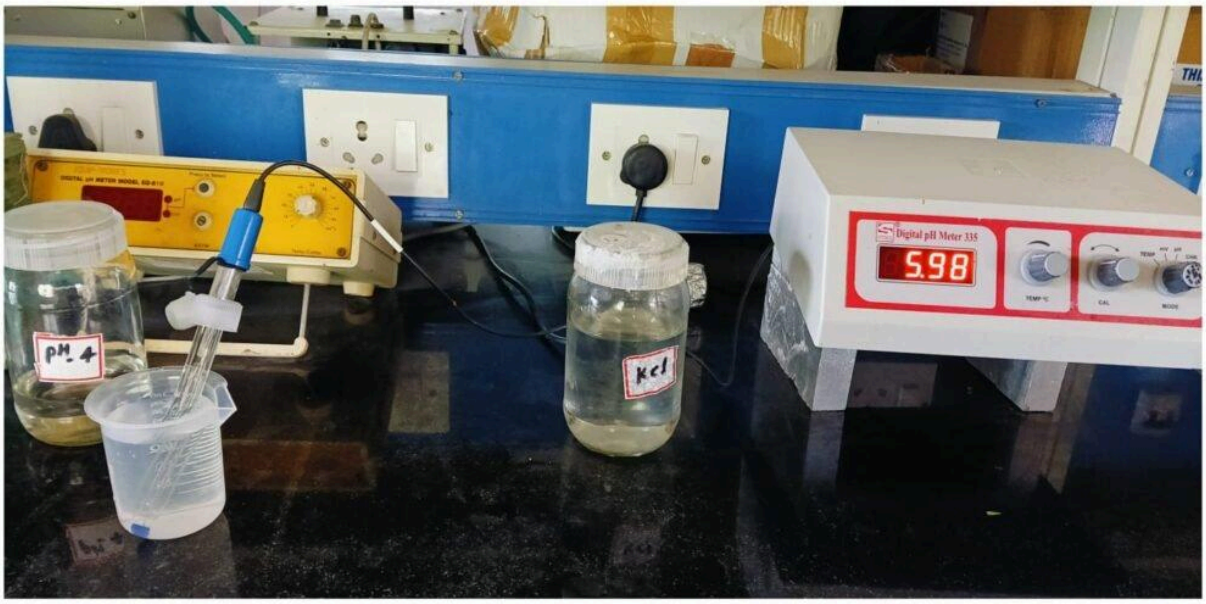

Fig. Measuring pH, EC and TDS of RO water

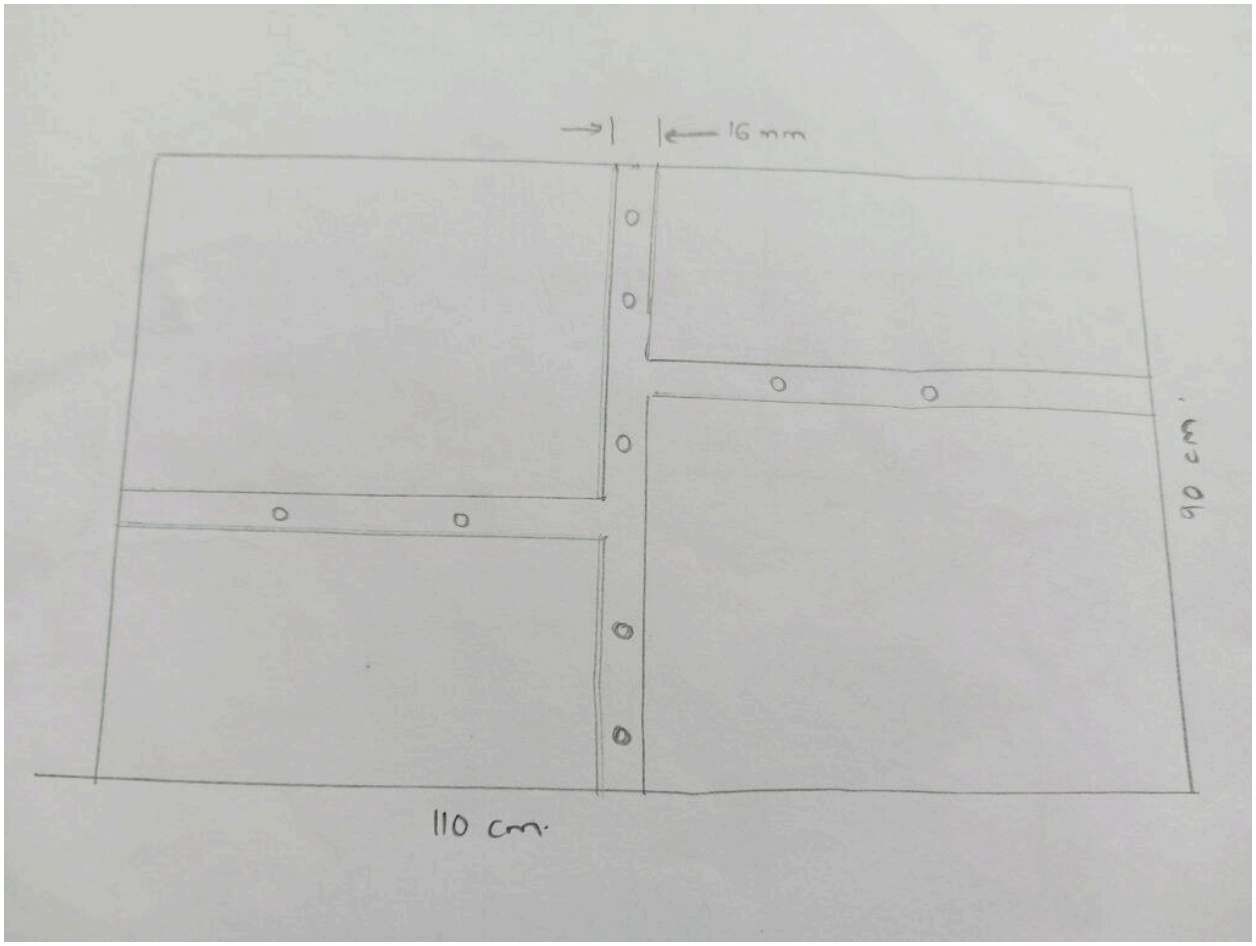

Experimental setup procedure :

1. A 1000-litre capacity IBC tank was selected and its top cover was cut open. The tank was then filled with 700 litres of RO water for the experiment, 1.47 kg of calcium sulfate ($CaSO_4$) was added to the water.
2. A cross-shaped (plus) structure made of lateral pipes was fabricated and mounted over the open top of the IBC tank for the installation of foggers. 9 foggers were installed for experiment.
3. 1 HP motor was connected to pump the solution from the tank through PVC piping into the lateral structure, enabling water delivery to the foggers.
4. With this, the experimental setup was completed. Now operate the foggers to get choke.

Fig. While cutting PVC pipe for preparing water supply connections

Fig. While fixing fogger structure over IBC tank

Fig. Experimental setup

Result:

The foggers were operated continuously for 8 hours per day. After 2–3 days, a reduction in mist output was observed. By the eighth day, the foggers were completely clogged, and white salt deposits were found. This marked the completion of the fogger clogging experiment.

fig. Salt accumulation on foggers. A blocked fogger

This experiment I have stopped here due completion of my fellowship tenure. Further experiment will be continued by next fellow or intern.

2.5 Treatment solutions for Algae formation on cooling pads

Due to the continuous dripping of water on the cooling pads, algae layers formed over time. These algae layers blocked the cooling pads, reducing their cooling efficiency. To address this issue, we designed an experiment to observe the impact of bleaching powder on algae growth.

Bleaching powder:

Parameter	Lime	Bleaching powder
Primary action	Increases pH to make environment less favorable.	Releases free chlorine, a strong oxidizer.
Effect on Algae	Slows growth by raising pH.	Kills algae by oxidizing cell component.
Speed of action	Slow and mild effect.	Fast and aggressive action.
Residual effect	Short-term	Long-term

To determine the effective dosage, calculated the amount of bleaching powder required for 15 liters of water. The ideal concentration of chlorine for algae control typically ranges between 1-5 gm/lit. Based on the active chlorine content in the bleaching powder, calculated the exact amount needed to achieve the desired concentration in 15 liters of water.

Calculations:

Available chlorine in Bleaching powder = 30-35 % (For safety consider 30%)

We want 100 ppm or 1 gm/lit concentration of chlorine.

Therefore, 0.1%

Required available chlorine = 15lit * 1 gm/lit

= 15 gm

Bleaching powder required = 15/0.30

= 50 gm

Based on calculations, prepared the treated water by adding the precise amount of bleaching powder to achieve the desired chlorine concentration. Once the powder was fully dissolved, poured the treated water into the bucket, ensuring the system was ready for operation. With the water in place, started the system, activating the pumps to circulate the treated water continuously over the cooling pads.

Another bucket filled with untreated water that is 15 litres of alga water

Setup for experiment

Treated water

Untreated water

Conclusion:

The experiment demonstrated the effectiveness of bleaching powder in controlling algae growth on cooling pads. By calculating and applying the optimal dosage, the treatment successfully reduced algae growth, maintaining system efficiency. The satisfactory results,, suggest that bleaching powder can be a viable solution for algae control in similar systems, offering a practical approach to improving performance and reducing maintenance needs.

Further study and experiment on this will be done by next fellow or intern working in this project.

Fig. Observation of both the pads

3.0 Energy Balance Model

3.1 Brief

We can use the previously gained insights of fogging on real microclimate facility to create an approximate but useful energy-balance model, that helps us size similar systems.

3.2 Mathematical Modelling

Here is the basic mathematical treatment of the model.

We consider a steady-state energy balance between solar heat gains and losses through the greenhouse cover. The key assumptions are:

- No active cooling or ventilation
- Clear sky, direct solar radiation
- Ground acts as a thermal sink at near-ambient temperature
- Negligible plant transpiration and internal heat sources

The simplified steady-state energy balance equation:

$$Q_{in} = Q_{out}$$

Where:

$$Q_{in} = \tau * I_{solar} * A_{proj}$$

$$Q_{out} = U * A_{cover} * (T_{in} - T_{out})$$

Here:

- τ is the transmissivity of HDPE cover (assumed 0.75)
- I_{solar} is the solar irradiance (W/m^2)
- A_{proj} is the projected area of the structure perpendicular to solar rays
- A_{cover} is the total surface area of the greenhouse cover
- U is the overall heat transfer coefficient ($W/m^2 \cdot K$)
- T_{in} and T_{out} are inside and outside air temperatures (°C)

Solving for internal temperature:

$$T_{in} = T_{out} + (\tau * I_{solar} * A_{proj}) / (U * A_{cover})$$

Humidity Estimation

Assuming a sealed enclosure with no added moisture sources, internal humidity is estimated by assuming absolute humidity remains constant while temperature rises:

$$AH_{out} = (RH_{out} / 100) * AH_{sat}(T_{out})$$

$$RH_{in} = 100 * AH_{out} / AH_{sat}(T_{in})$$

Where $AH_{sat}(T)$ is the saturation absolute humidity at temperature T, calculated from psychrometric relationships (Clausius–Clapeyron).

Role of Geometry (V/A Ratio)

The enclosure shape directly affects internal climate because:

- Surface area influences heat loss (higher A_{cover} → greater cooling)
- Projected area influences solar gains (higher A_{proj} → more absorbed energy)
- The Volume-to-Surface-Area ratio (V/A) is a useful metric; higher V/A indicates more thermal mass per unit surface, reducing temperature swings.

We modeled variations:

- Dome vs. flat-roof box shapes
- Tall slender vs. low wide enclosures
- Different azimuth orientations

Sample Results

Case studies at 13:00 on May 15 for Pabal, Pune:

This is done for the real geometry, as exists at Pabal.

Inputs used:

- $G = 1000\ \mathrm{W/m^2}$ (mid-day clear sky),
- $A_{roof} = 64\ \mathrm{m^2}$,
- $\tau = 0.75 \rightarrow Q_{solar,in} = 1000 \times 64 \times 0.75 = 48{,}000\ \mathrm{W}$.
- $U = 6.0\ \mathrm{W/m^2 \cdot K}$,
- $A_{cover} = 256\ \mathrm{m^2}$,
- $T_{out} = 37.0\ ^\circ\mathrm{C}$.

Compute steady-state:

$$\Delta T = \frac{Q_{solar,in}}{U A_{cover}} = \frac{48{,}000}{6.0 \times 256} \approx 31.3\ ^\circ\mathrm{C}.$$

So

$$T_{in} \approx 37.0 + 31.3 \approx \mathbf{68.3\ ^\circ C}.$$

Actual measured temperature inside the dome was 65 deg. C. in Summer.

- Dome (same volume, smaller surface area) can intercept more sunlight due to larger projected area, yielding much higher internal temperatures (~99 °C).

Here is a sweep graph of the same mathematical equations, but various V/A ratios.

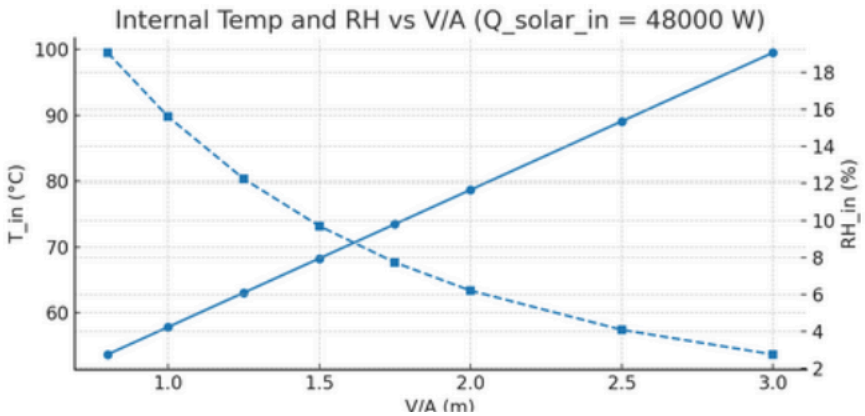

- Flat box designs show lower peak temperatures (~75 °C) under identical assumptions.
- Orientation matters more for elongated boxes, with optimal solar gain azimuth varying by time of day.

Greenhouse Energy Balance with Fogging (Evaporative Cooling)

This revision extends the steadystate greenhouse energy balance to include fogging. Fogging is modeled as an evaporation mass flow rate (L/h), which adds moisture to the air while extracting latent and sensible heat from the indoor air. The result is lower air temperature and higher humidity.

1) Governing Energy Balance

Let the projected area toward the sun be A_proj, the total cover area be A_cover, and the overall heat transfer coefficient be U. With fogging mass flow $\dot{m}_f$ (kg/s) evaporated into the space, the steady energy balance is:

$$\tau \cdot I \cdot A_{proj} = U \cdot A_{cover} \cdot (T_{in} - T_{out}) + \dot{m}_f \cdot [\, h_{fg}(T_{in}) + c_w \cdot (T_{in} - T_w) \,]$$

Solving for T_in:

$$T_{in} = \{ \tau \cdot I \cdot A_{proj} + U \cdot A_{cover} \cdot T_{out} + \dot{m}_f \cdot c_w \cdot T_w - \dot{m}_f \cdot h_{fg}(T_{in}) \} / \{ U \cdot A_{cover} + \dot{m}_f \cdot c_w \}$$

For practical use over a narrow temperature range, h_fg(T_in) can be treated as constant (≈ 2.43 MJ/kg near 35–40 °C).

Terms:

τ is cover transmissivity;
I is solar irradiance (W/m²);
A_proj is the projected area normal to sun;
A_cover is the total cover area;
U is overall heat transfer coefficient;
T_in/T_out are indoor/outdoor air temperatures;
$\dot{m}_f$ is evaporation rate (kg/s);
h_fg is latent heat of vaporization;
c_w is water specific heat;
T_w is water supply temperature.

2) Moisture Balance and Humidity

In the noventilation snapshot, fogging adds water vapor to the air volume V. Using absolute humidity μ (kg_vapor per m³):

$$d\mu/dt = \dot{m}_f / V$$

Given temperature T_in, the water vapor partial pressure is $e = \mu \cdot R_v \cdot T_K$ (R_v = 461.5 J/kg·K), and relative humidity RH = e / e_s(T_in), where e_s(T) is saturation vapor pressure. In practice, evaporation slows as RH → 100%; models should cap evaporation or route excess liquid to drainage.

5. Conclusion

This simplified model demonstrates that greenhouse geometry, orientation, and cover properties strongly influence internal microclimate. Real-world conditions would require accounting for ventilation, shading, evapotranspiration, and thermal mass for accurate prediction. However, even a simplistic model as prepared, can be used to gauge critical insights towards sizing of system.